Evidence for new resonances

in the combined analysis of recent hyperon photoproduction data

V.A. Nikonov (HISKP, Uni-Bonn; PNPI, Gatchina)

- **PWA group in HISKP:**

  A.Anisovich, E.Klempt, V.Nikonov, A.Sarantsev, U.Thoma

  (http://pwa.hiskp.uni-bonn.de)

- **Approach and recent results were presented in the talk of A.Anisovich**

- **The main task: search for new baryon resonances**
  - **Polarization data are sensitive to weak signals**
  - **Double polarization is necessary for a complete experiment**
  - **CB ELSA double polarization data taking started**

    (talks of U.Thoma and R.Beck)

$N(2070)D_{15}$ **was discovered in combined fit of** η **and** π^0 **photoproduction.**

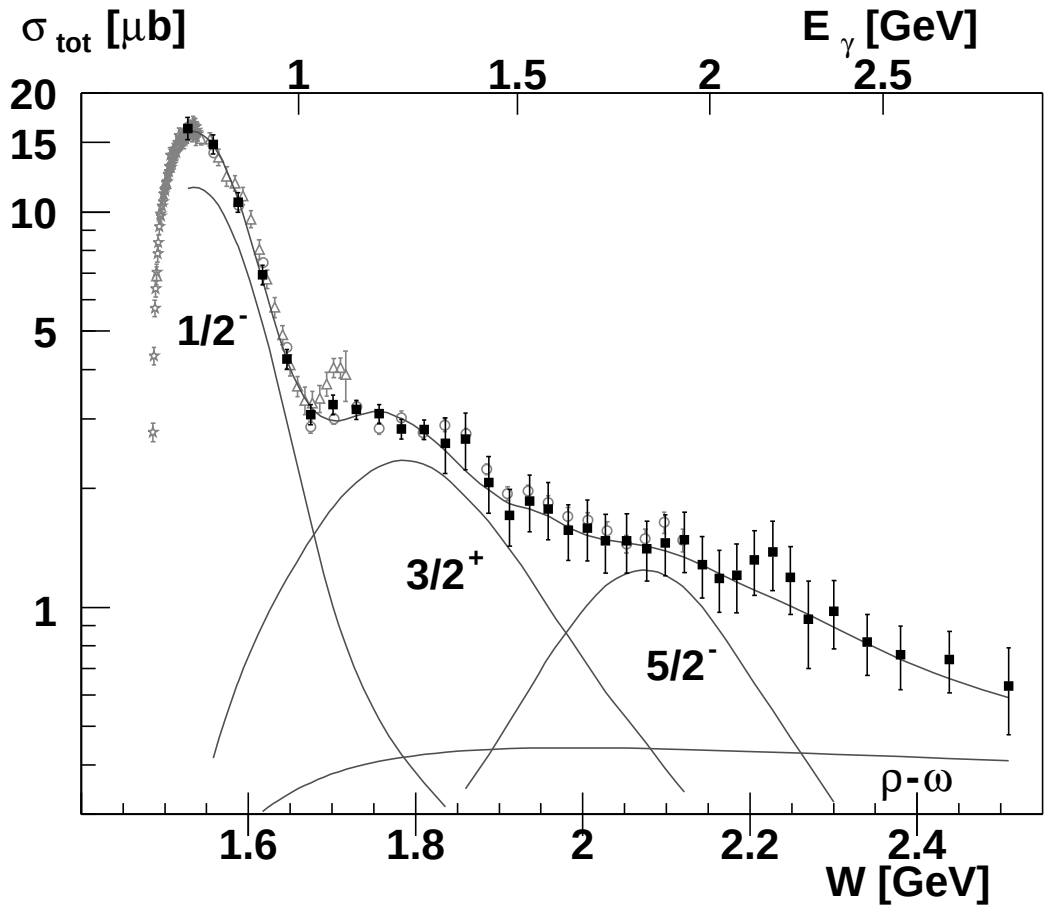

The check can be made using double polarization data.

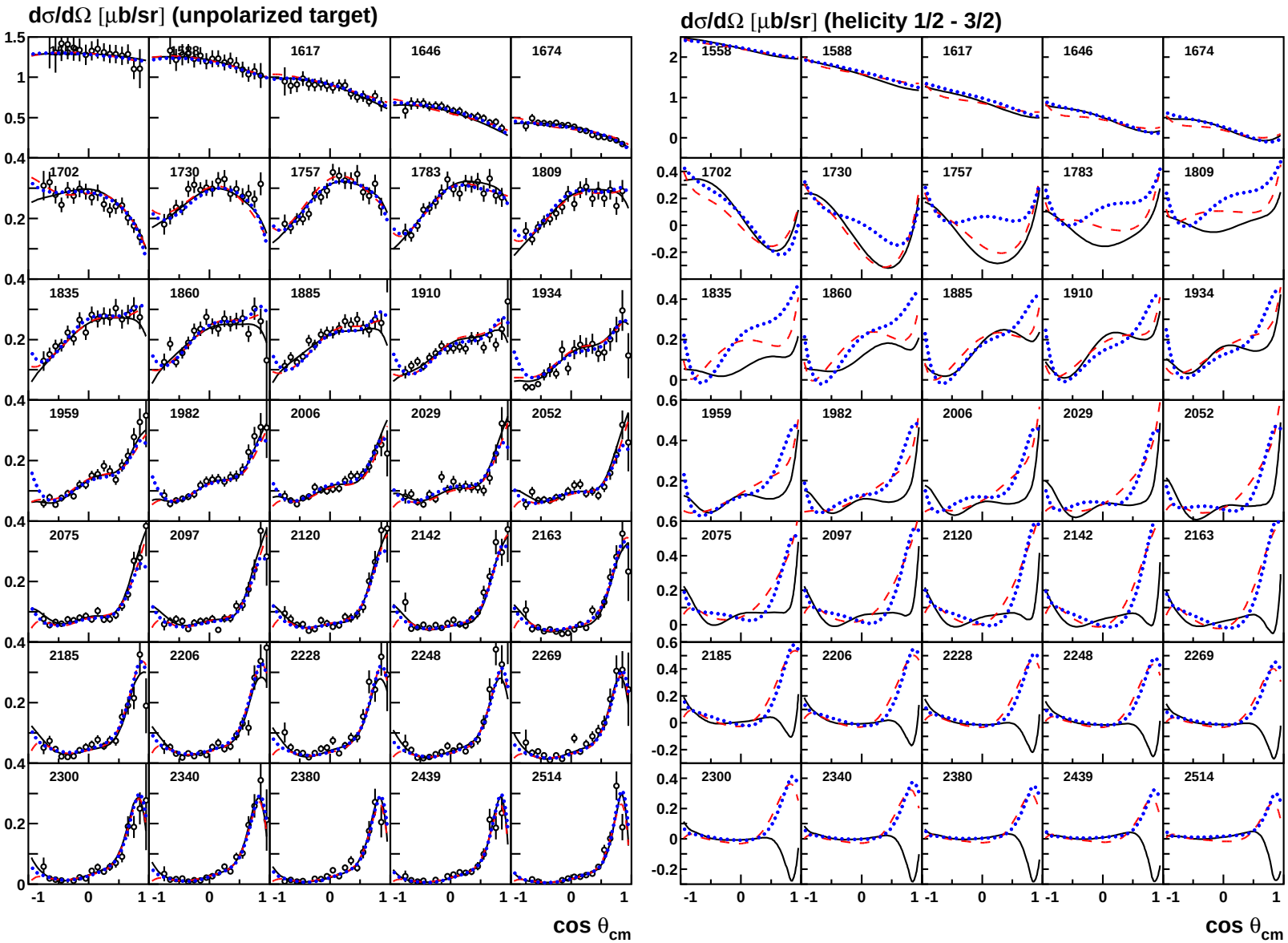

$N(2070)D_{15}$ **substituted with** $1/2^-$ **or with a** $1/2^+$

The P_{11}(1840) and P_{13}(1900) states

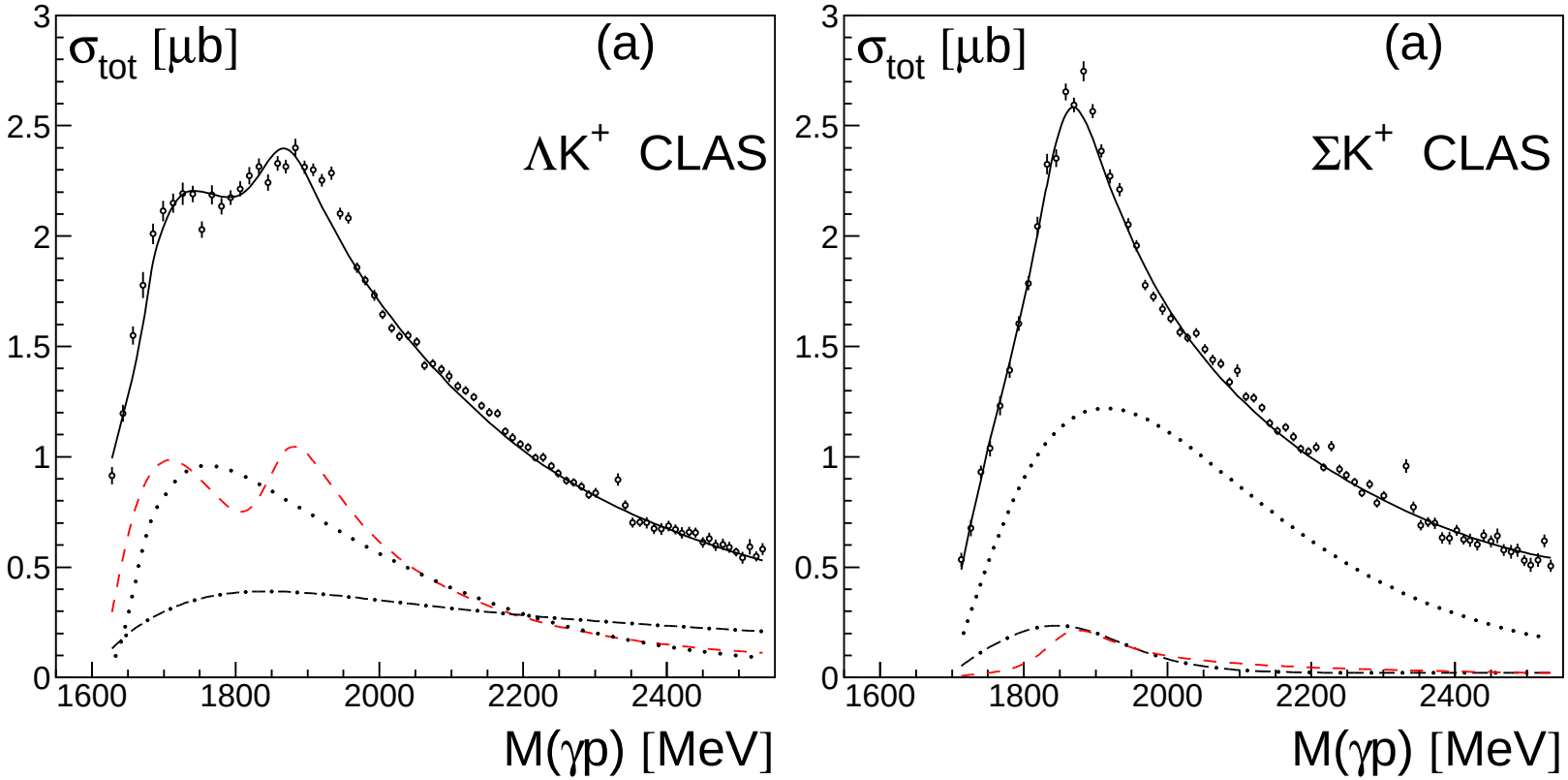

A relatively narrow resonance is needed in 1850-1900 MeV region

$\gamma p \to \Lambda K^+$: **dashed** P_{13}**, dotted** S_{11}**, dash-dotted** K^* **exchange.**

$\gamma p \to \Sigma K^+$: **dashed** P_{13}**, dash-dotted** P_{11}**, dotted** K **exchange.**

The main proof is $K^0\Sigma^+$

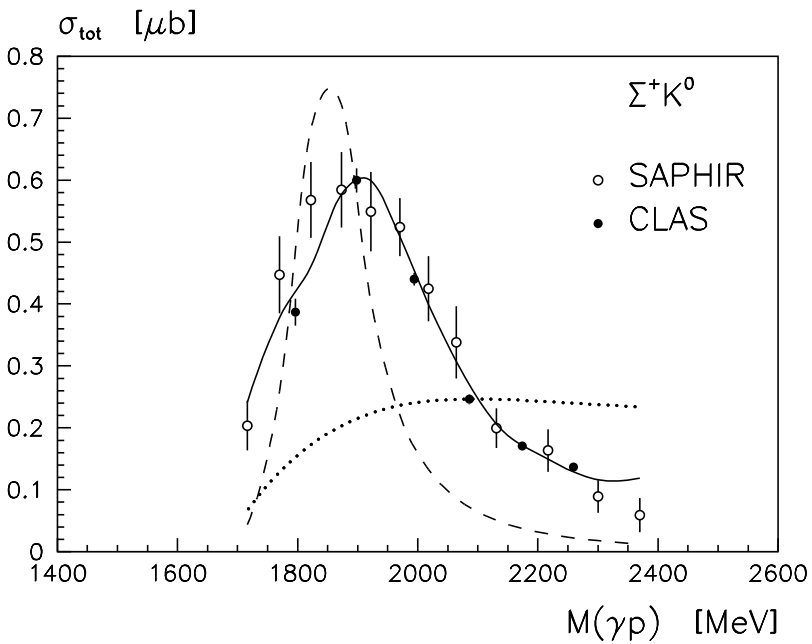

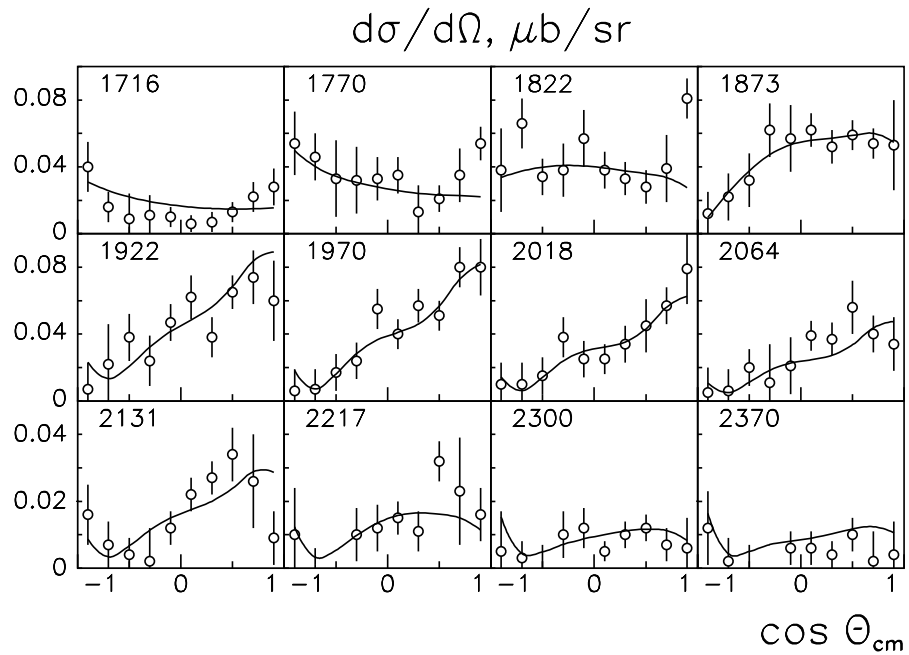

dashed P_{11}(1840)

P_{11} **gives the best** χ^2

P_{13} **gives the second best** χ^2

Could be both, but with pure data it is not a proof.

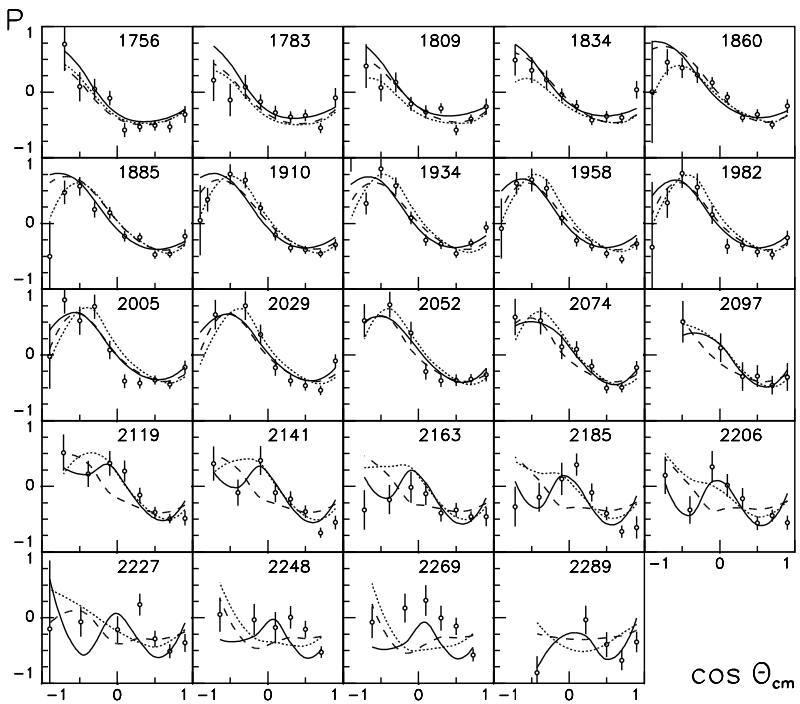

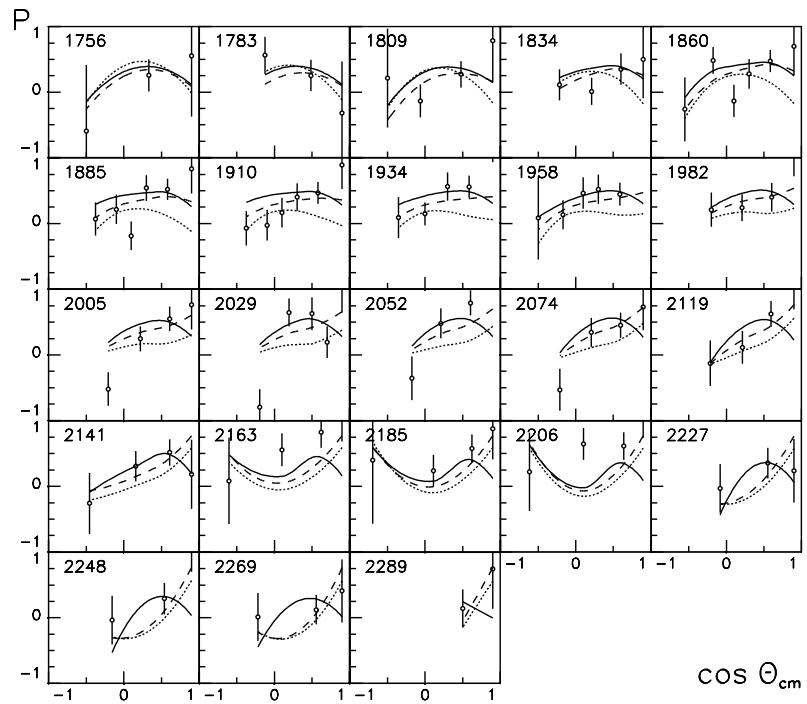

ΛK^+ **(left) and** ΣK^+ **(right) recoil polarization (CLAS)**

Dotted line is the fit without $P_{11}(1840)$

New C_x, C_z data:

Evidence for the $N(1900)P_{13}$

No model could describe them.

In our approach we also had no good description of C_x, C_z with old set of resonances.

Systematic discrepancies were observed.

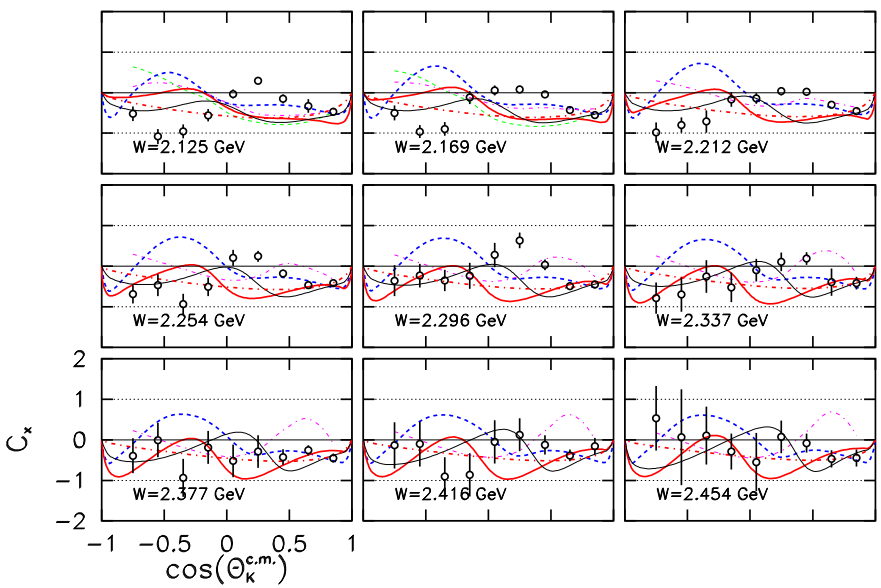

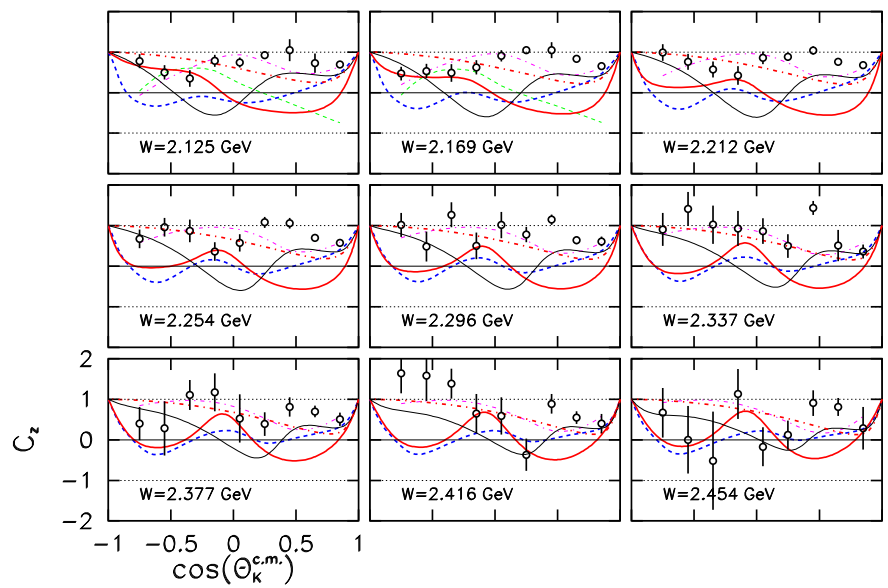

Refit of new data with old resonances. Maximal freedom for non-resonance contributions.

Description of other data is much worse than before.

We tried to add new resonances.

As the firsr step, further resonances were introduced as Breit-Wigner amplitudes and different quantum numbers were tested.

The best χ^2 was obtained by introducing the second P_{13} state.

Solution 1: 1885 ± 15 **MeV mass and** 180 ± 25 **MeV width, with** $\Delta\chi^2 = 1540$**.**

Solution 2: 1975 ± 15 **MeV mass and** 200 ± 20 **MeV width.**

Replacing:

S_{11} $\Delta\chi^2$ **= 950.**

D_{15} $\Delta\chi^2$ **= 970.**

P_{11} $\Delta\chi^2$ **= 205.**

F_{15} $\Delta\chi^2$ **small.**

P_{33} $\Delta\chi^2$ **smaller by a factor 2 than for a** P_{13}**.**

F_{17}, G_{17} **did not improve the fit.**

In a final step, the P_{13} was parameterized as 3-pole 8-channel K-matrix with πN, ηN, $\Delta(1232)\pi$ (P and F-waves), $N\sigma$, $D_{13}(1520)\pi$ (S-wave), $K\Lambda$ and $K\Sigma$ channels.

This resulted in the fit solutions 1 and 2 which both are compatible with B-W fits.

In addition, both solutions are compatible now with elastic πN scattering.

From the fit, properties of resonances in the P_{13}-wave were derived.

The lowest-mass pole is identified with the established $N(1720)P_{13}$,

the second pole with the badly known $N(1900)P_{13}$.

The third pole is introduced at about 2200 MeV.

It improves the quality of the fit in the high-mass region but its quantum numbers cannot be deduced safely from the present data base.

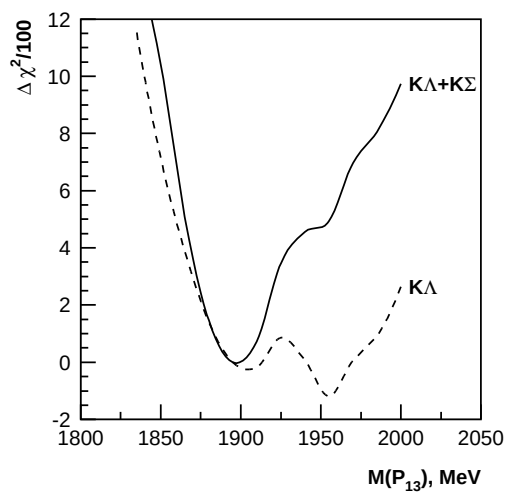

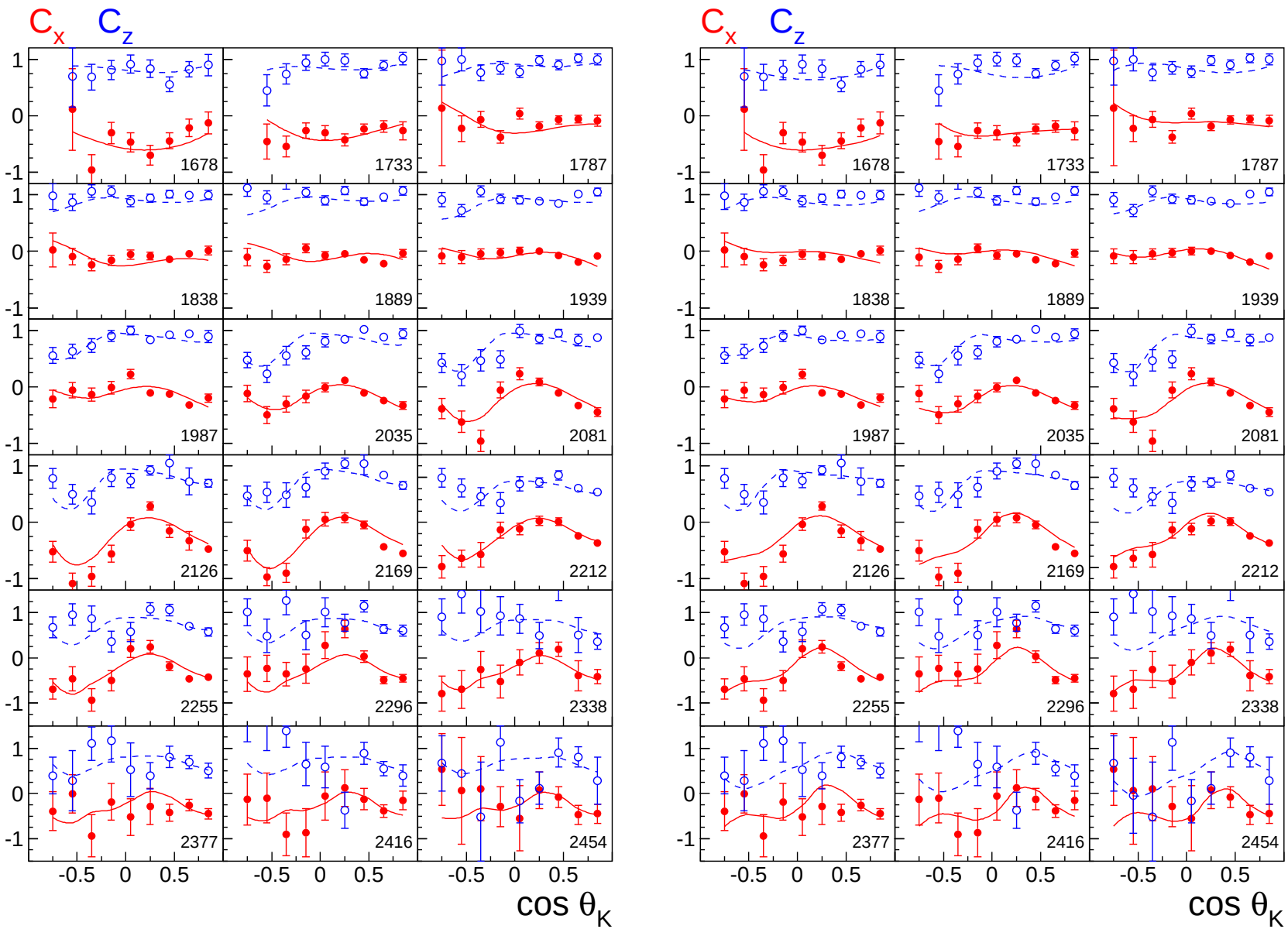

C_x **(full circles) and** C_z **(open circles) for** $\gamma p \to \Lambda K^+$**. The solid and dashed curves are results of our fit obtained with solution 1 (left) and solution 2 (right) for** C_x **and** C_z**.**

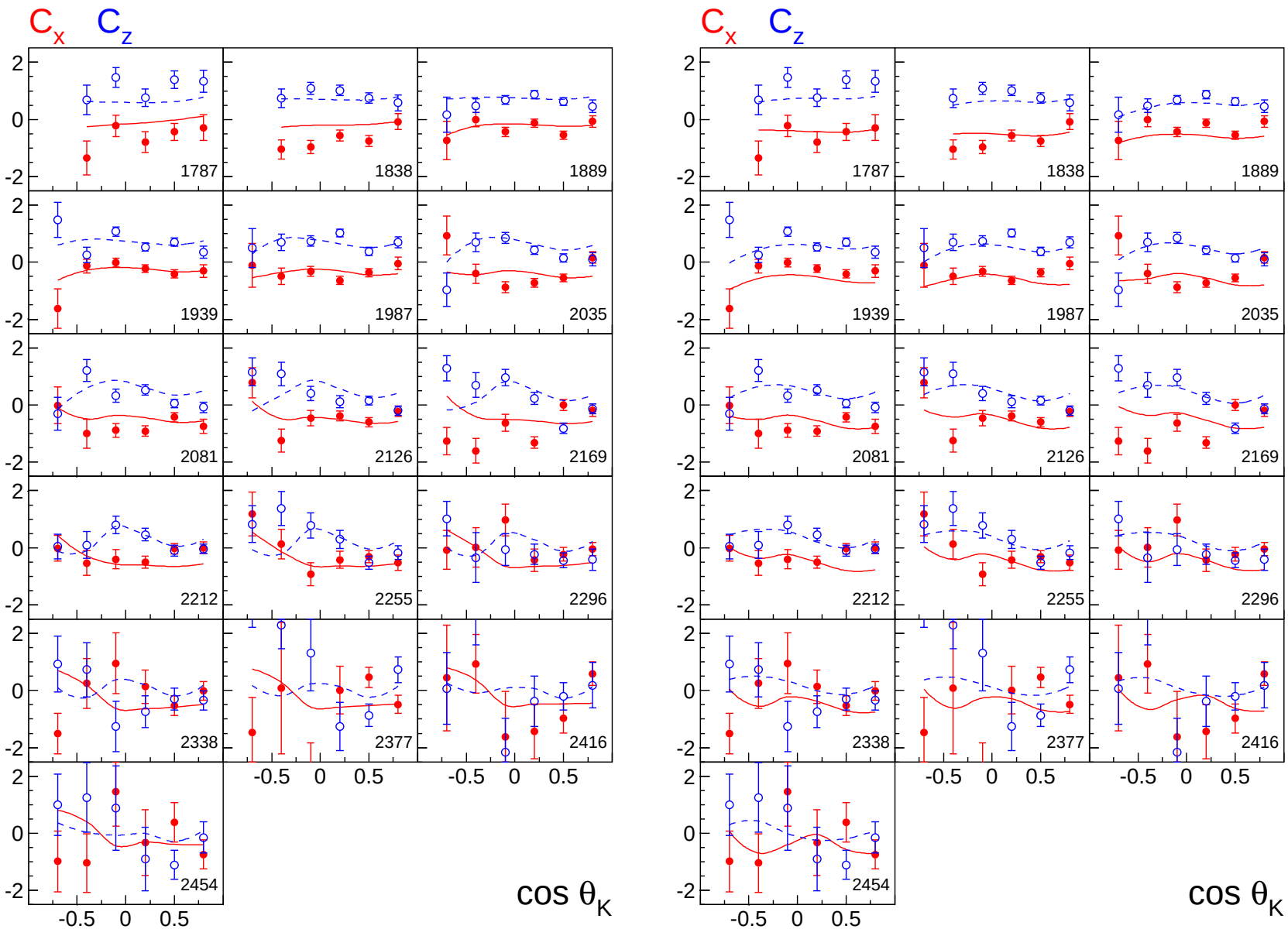

C_x (full circles) and C_z (open circles) for $\gamma p \to \Sigma K^+$. The solid and dashed curves are results of our fit obtained with solution 1 (left) and solution 2 (right) for C_x and C_z.

$\sigma_{tot}(\gamma p \to K^0\Sigma^+)$ from CB-ELSA

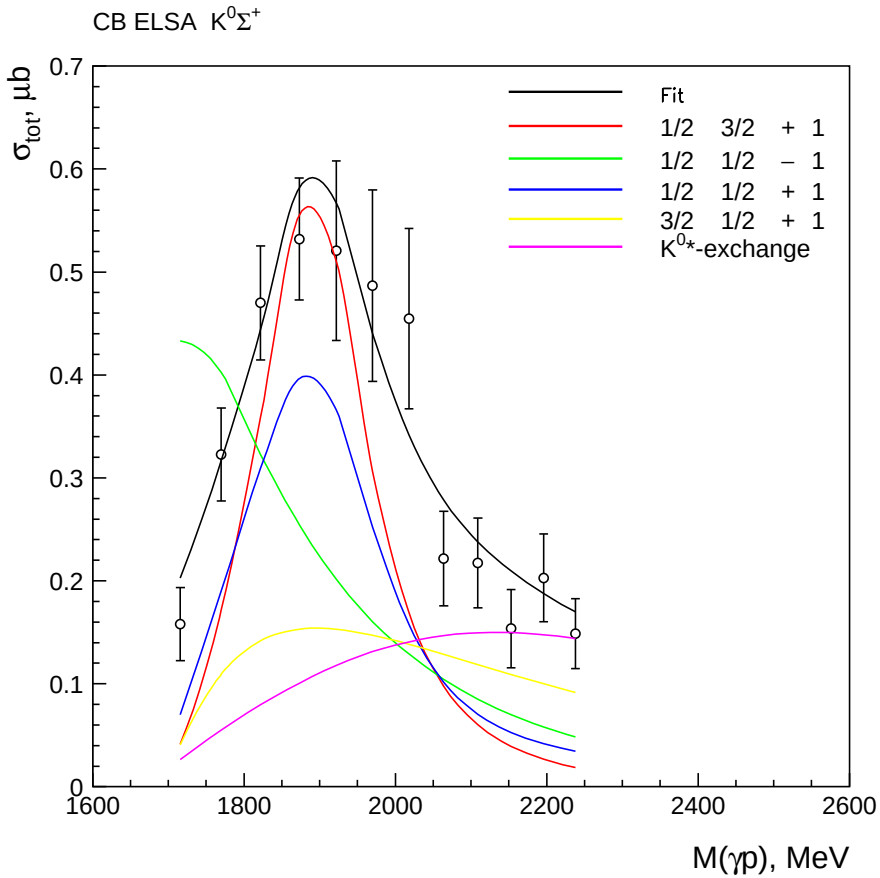

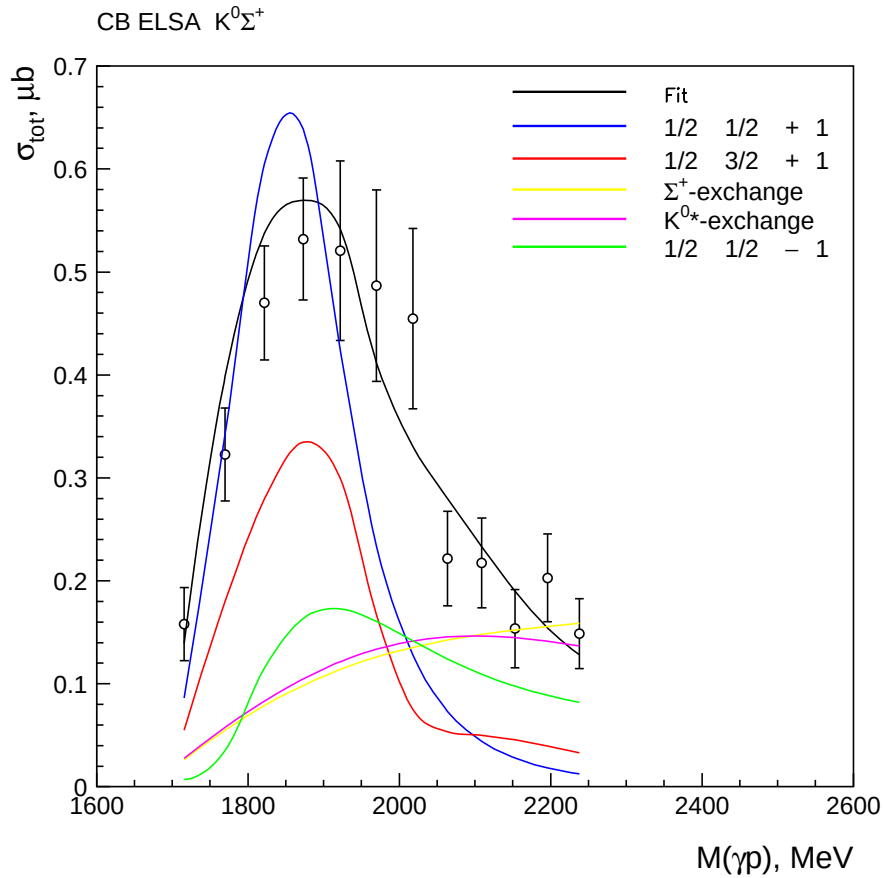

Red line – $P_{13}(1900)$

Blue line – $P_{11}(1860)$ **(improved** P **in** $K\Lambda$ **and** $K\Sigma$ **data)**

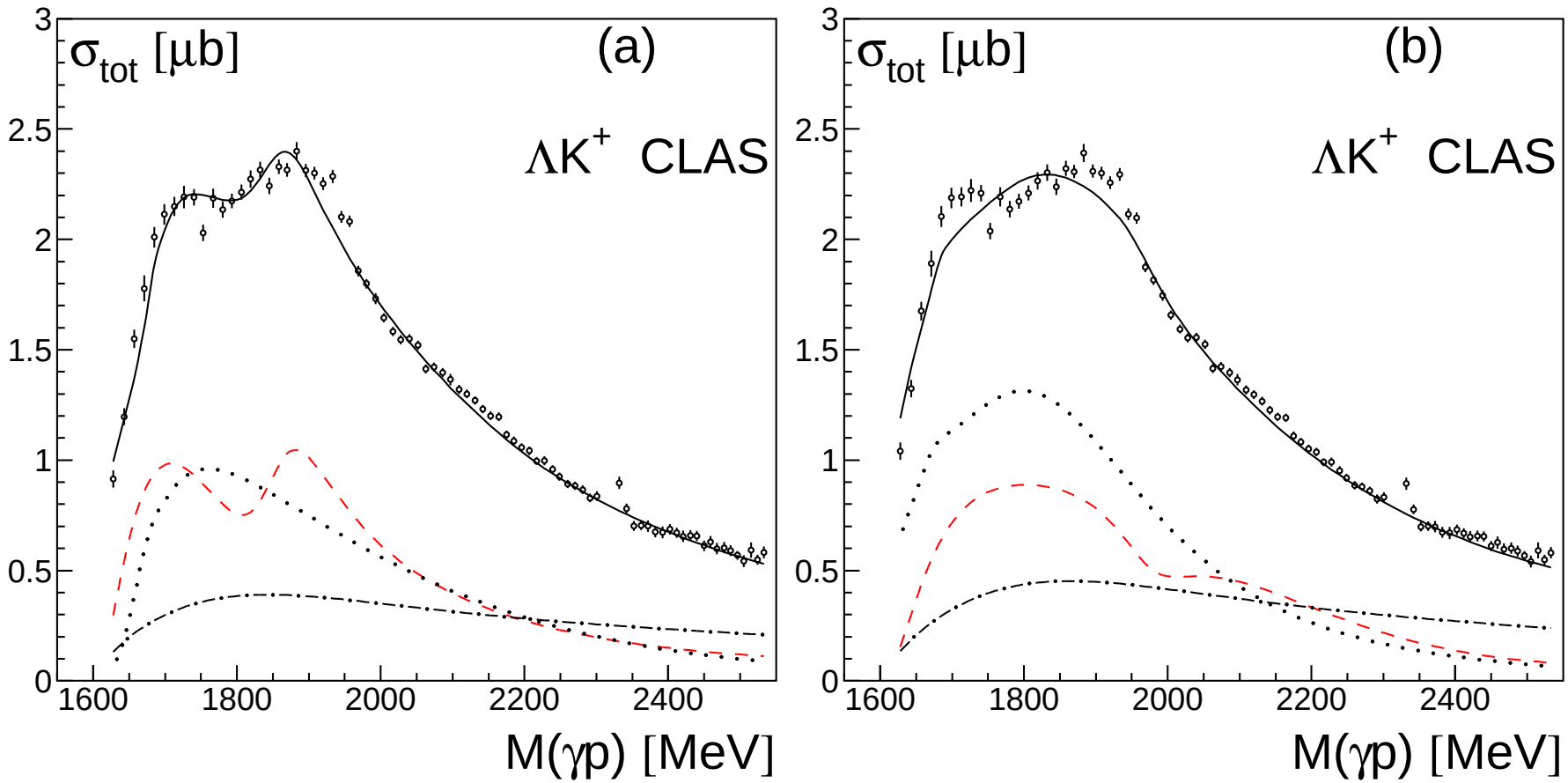

The total cross section for $\gamma p \to \Lambda K^+$ for solution 1 (a) and solution 2 (b). The solid curves are the results of our fits, dashed lines are the P_{13} contribution, dotted lines are the S_{11} contribution and dash-dotted lines are the contribution from K^* exchange.

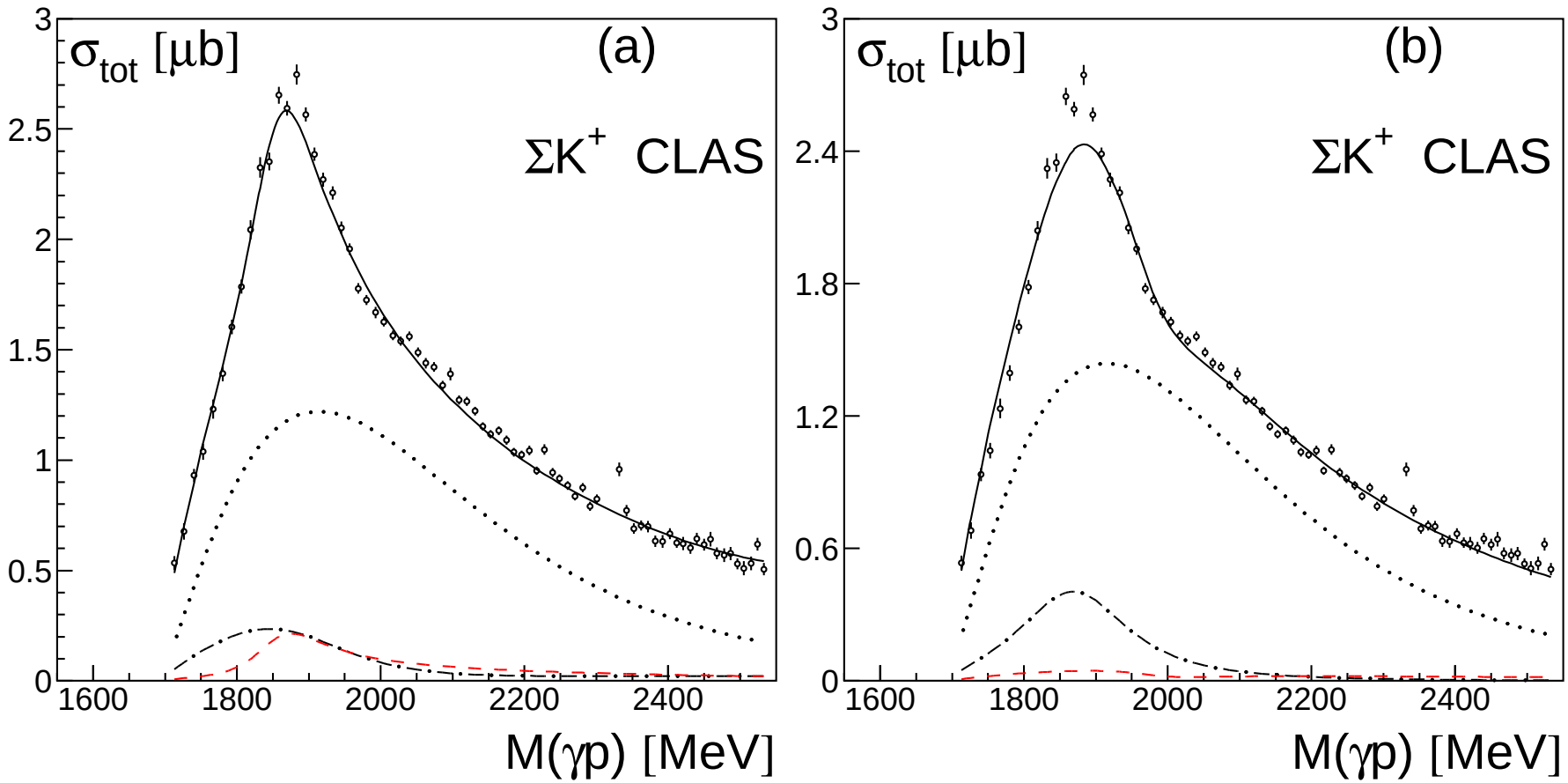

The total cross section for $\gamma p \to \Sigma K^+$ for solution 1 (a) and solution 2 (b). The solid curves are the results of our fits, dashed lines are the P_{13} contribution, dash-dotted lines are the P_{11} contribution and dotted lines are the contribution from K exchange.

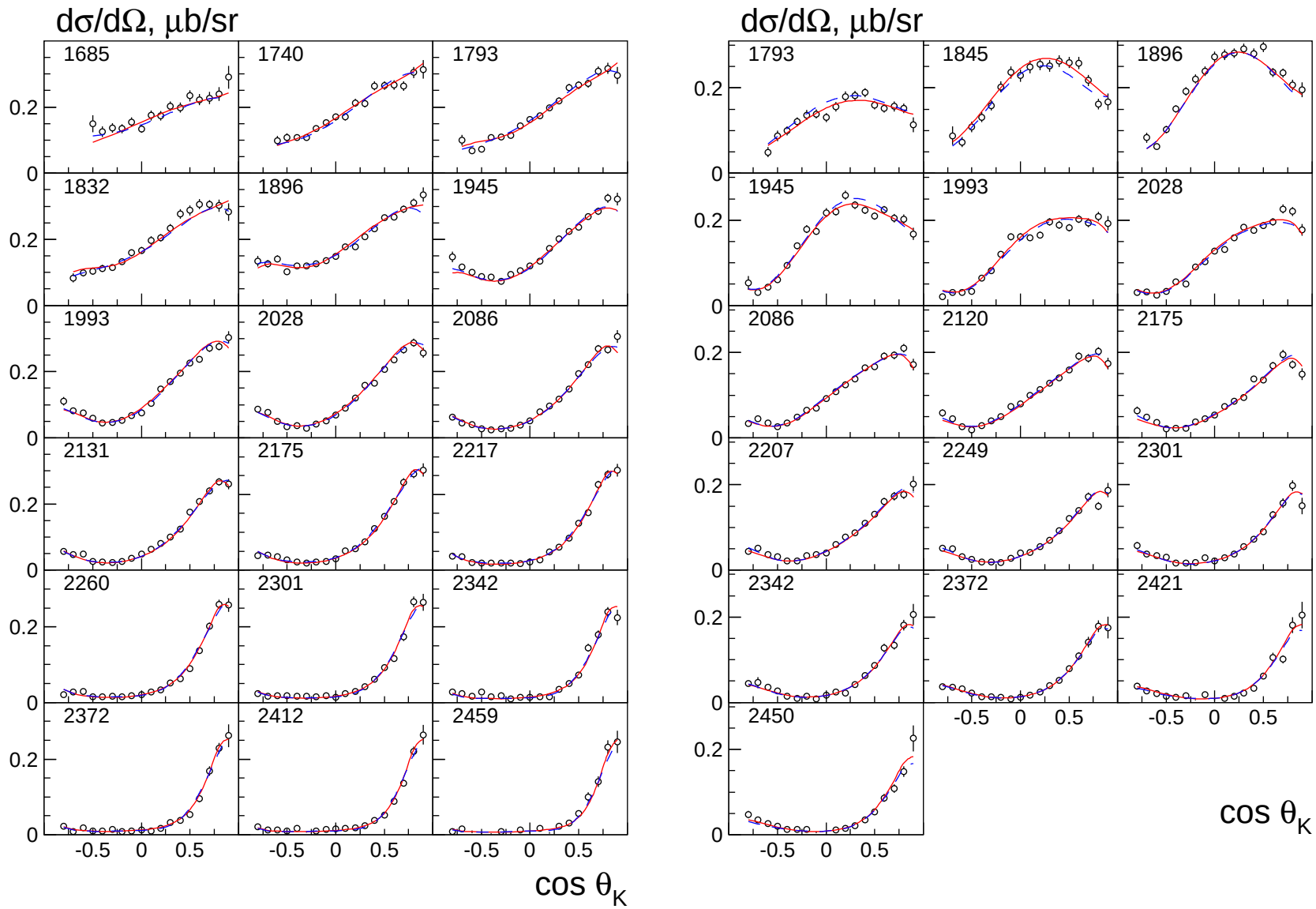

$\gamma p \to \Lambda K^+$ **(left) and** $\gamma p \to \Sigma K^+$ **(right). Only energy points where** C_x **and** C_z **were measured are shown. The solution 1 is shown as solid line and solution 2 (hardly visible since overlapping) as a dashed line.**

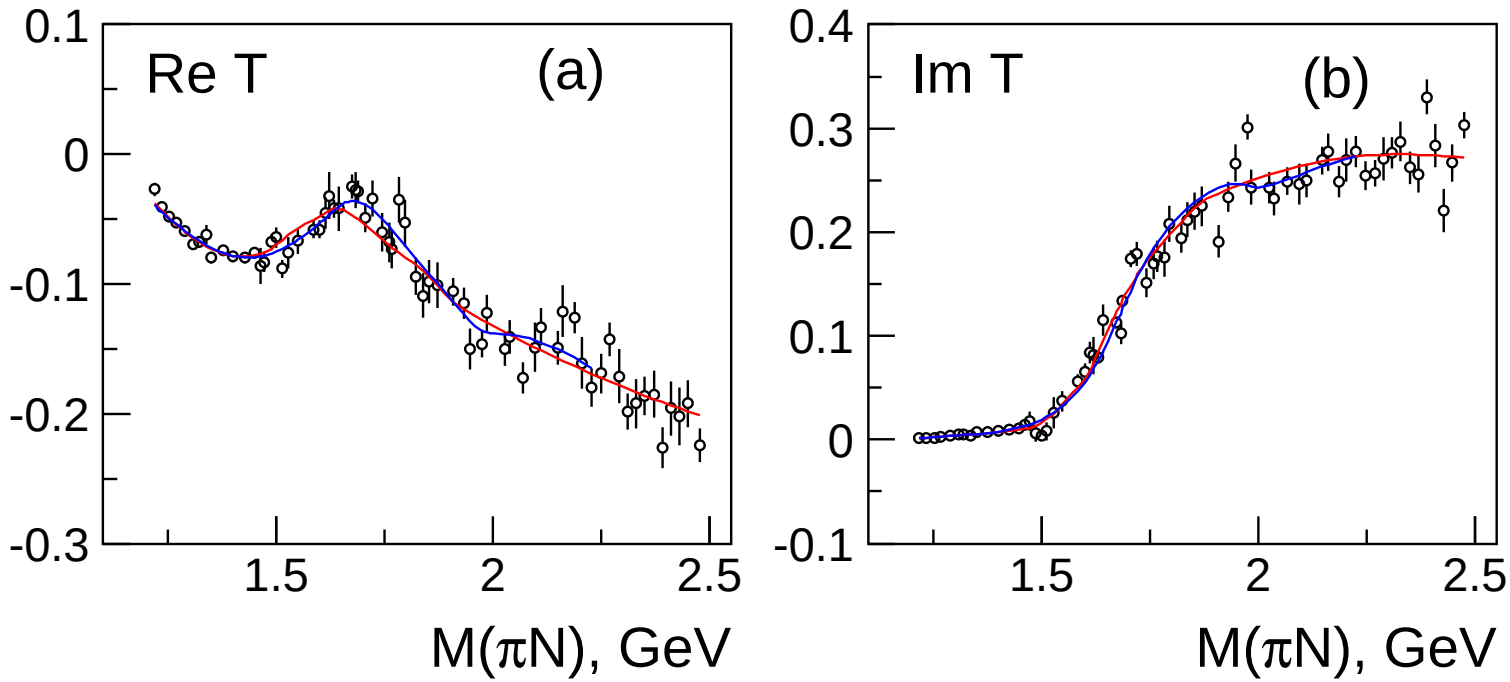

Real (a) and imaginary (b) part of the P_{13} elastic scattering amplitude

solution 1 and solution 2

Polarization variables are related as: $C_x^2 + C_z^2 \leq \mathrm{Min}((1-\Sigma^2),(1-P^2))$

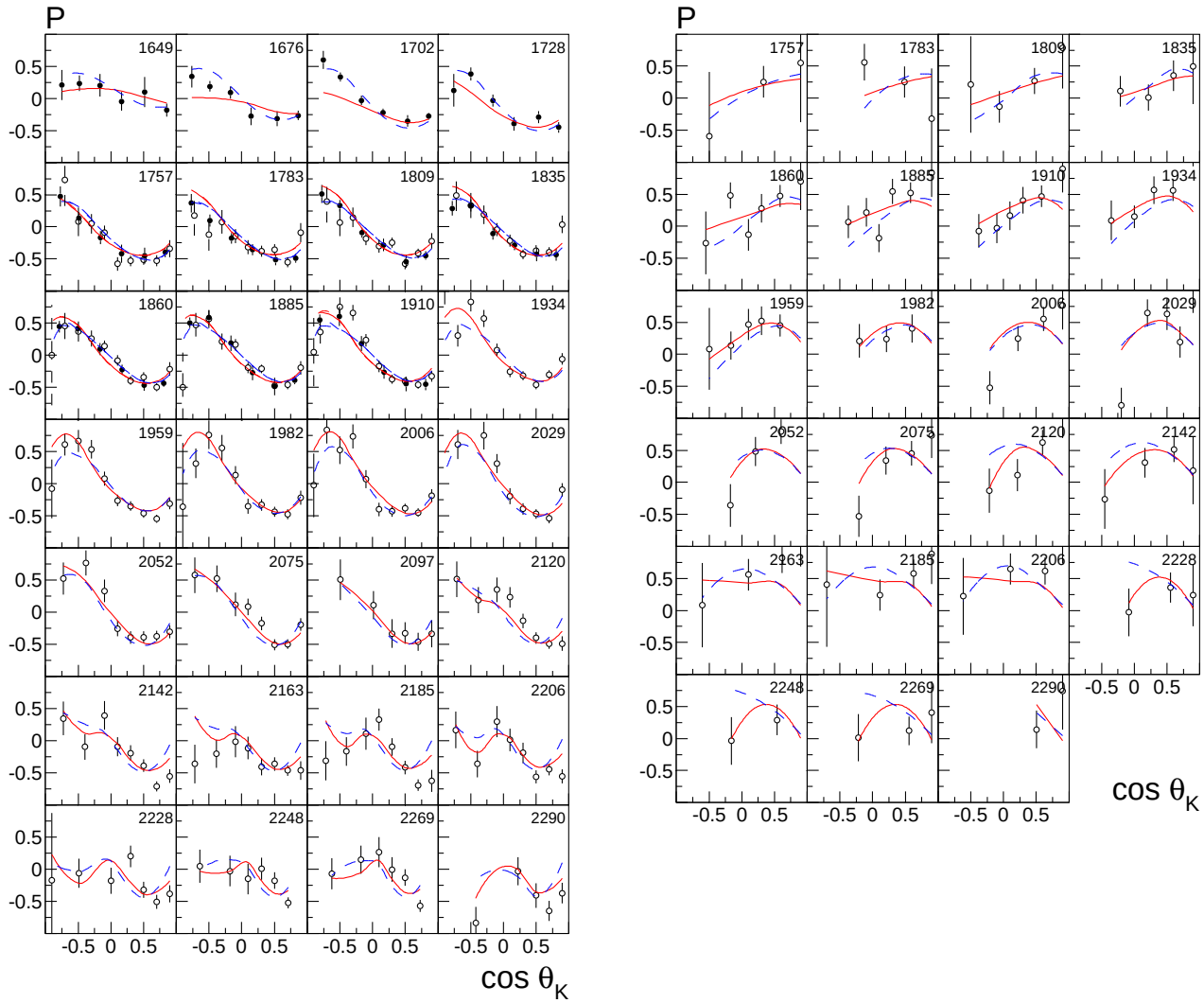

$\gamma p \rightarrow K^+\Lambda$ **(left) and** $\gamma p \rightarrow K^+\Sigma^0$ **(right) from CLAS (open circle) and GRAAL (black circle).**

The solid and dashed curves are solution 1 and 2 respectively.

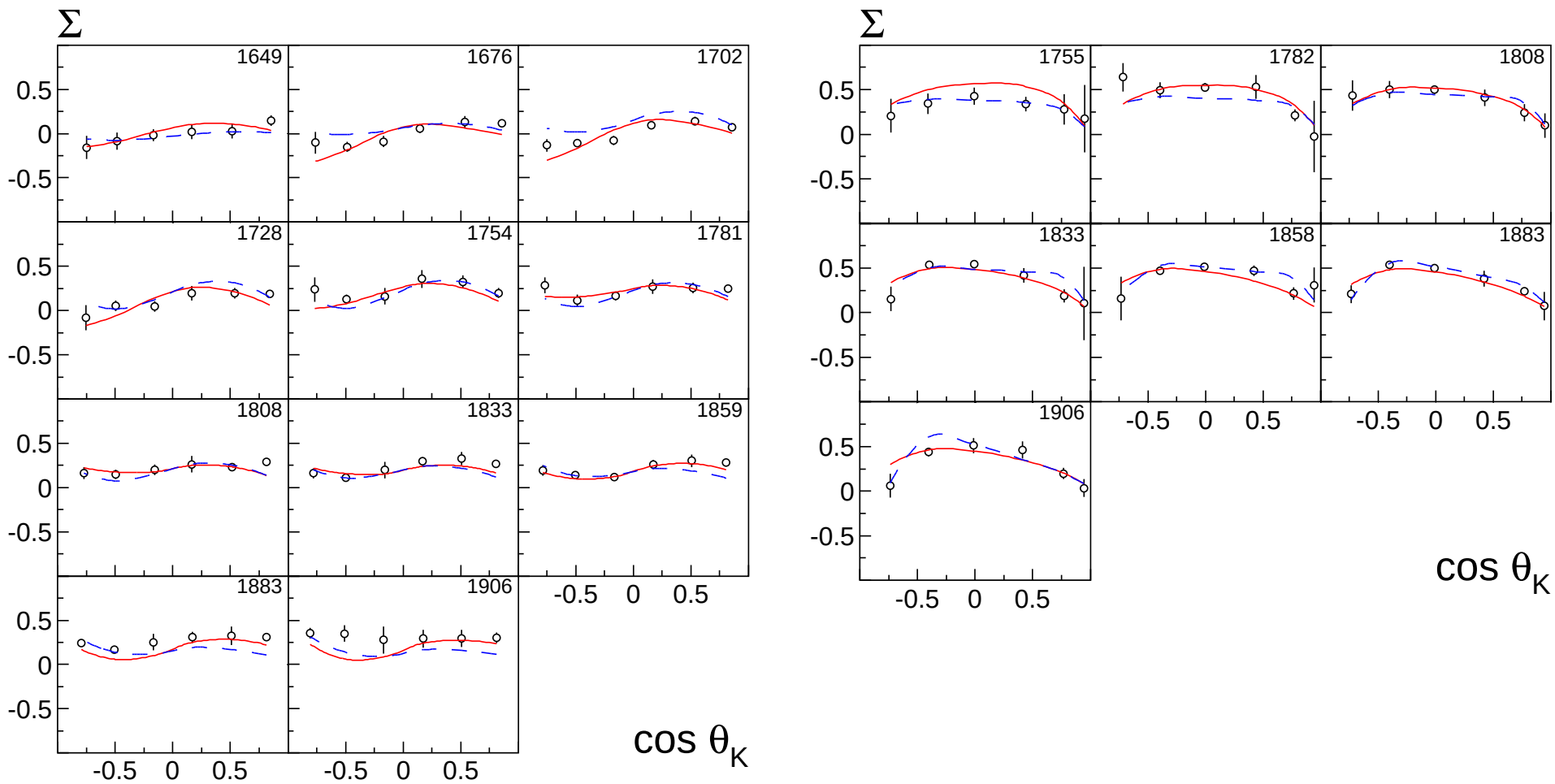

The beam asymmetries as a function of W for $\gamma p \to K^+\Lambda$ (left) and $\gamma p \to K^+\Sigma$ (right). The solid and dashed curves are the result of our fit obtained with solution 1 and 2, respectively.

The masses, widths are given in MeV, the branching ratios in % and helicity couplings in 10^{-3} GeV$^{-1/2}$. The helicity couplings and phases were calculated as residues in the pole position.

	Solution 1		Solution 2	
M_{pole}	1640 ± 80	1870 ± 15	1630 ± 60	1960 ± 15
Γ_{tot}^{pole}	480 ± 60	170 ± 30	440 ± 60	195 ± 25
M_{BW}	1800 ± 100	1885 ± 15	1780 ± 80	1975 ± 15
Γ_{tot}^{BW}	700 ± 100	180 ± 25	680 ± 80	200 ± 25
$A_{1/2}$	140 ± 80	$-(15 \pm 15)$	160 ± 40	$-(18 \pm 8)$
$\varphi_{1/2}$	$-(10 \pm 15)^\circ$	–	$(10 \pm 15)^\circ$	$(40 \pm 15)^\circ$
$A_{3/2}$	150 ± 80	$-(40 \pm 15)$	70 ± 30	$-(35 \pm 12)$
$\varphi_{3/2}$	$-(40 \pm 30)^\circ$	$-(20 \pm 15)^\circ$	$(0 \pm 20)^\circ$	$-(40 \pm 15)^\circ$
$\mathrm{Br}_{N\pi}$	8 ± 4	5 ± 3	11 ± 4	6 ± 3
$\mathrm{Br}_{N\eta}$	13 ± 4	21 ± 8	5 ± 2	15 ± 3
$\mathrm{Br}_{\Delta\pi(P)}$	48 ± 10	3 ± 2	28 ± 6	7 ± 2
$\mathrm{Br}_{\Delta\pi(F)}$	2 ± 2	4 ± 3	11 ± 4	21 ± 5
$\mathrm{Br}_{K\Lambda}$	15 ± 6	10 ± 5	5 ± 2	12 ± 3
$\mathrm{Br}_{K\Sigma}$	< 1	20 ± 8	< 1	8 ± 2
$\mathrm{Br}_{D_{13}\pi}$	10 ± 6	8 ± 3	38 ± 6	5 ± 3
$\mathrm{Br}_{N\sigma}$	4 ± 2	30 ± 12	2 ± 2	26 ± 8

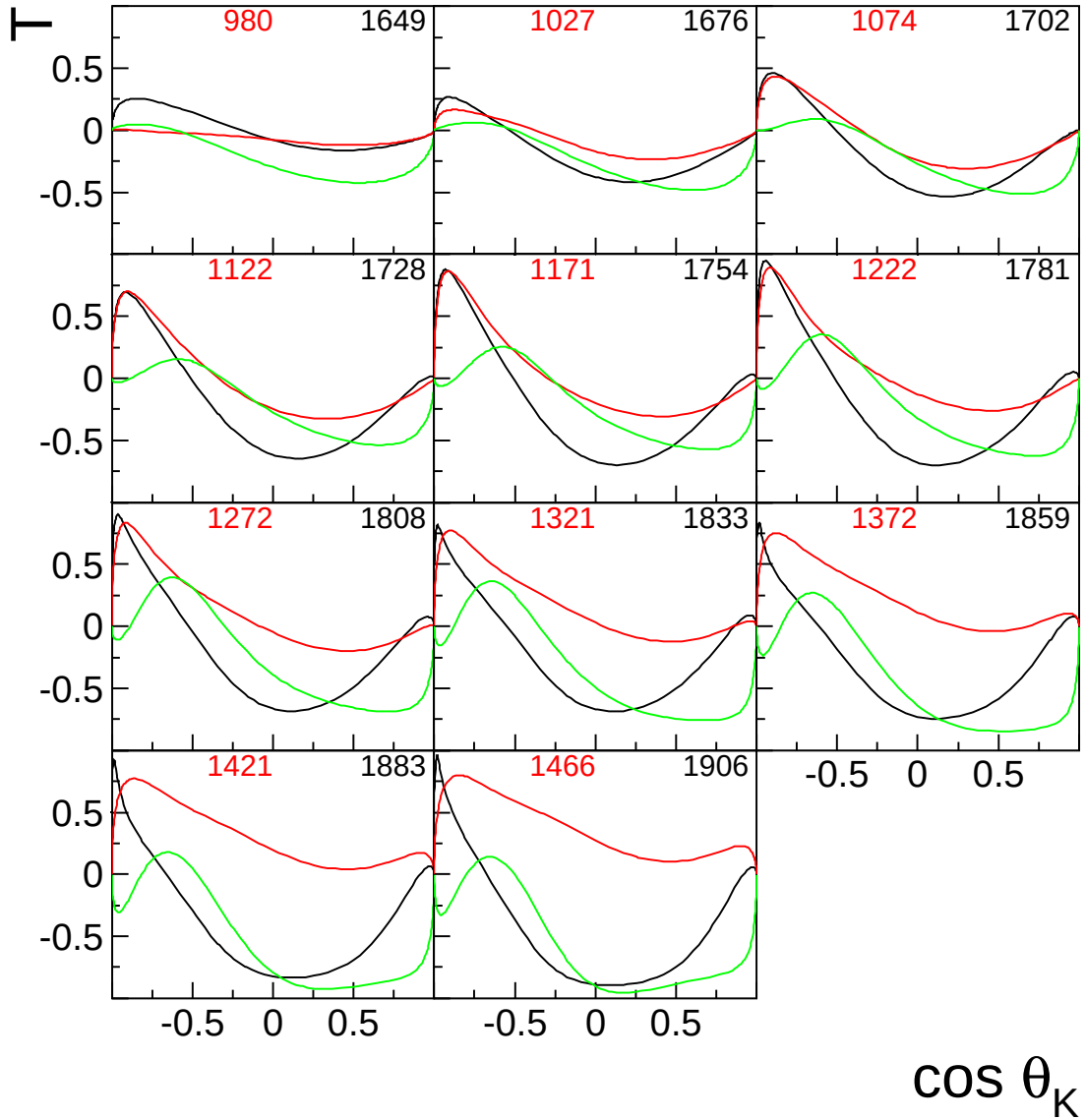

Predictions for T polarization.

Could be possible to choose between three solutions.

Conclusions

- **New P_{13} state has found fitting new CLAS C_x, C_z data**
- **A qualitatively good description of all fitted observables was obtained.**
- **The analysis of the first double polarization data on hyperon photoproduction reveals an exciting result.**
- **Systematic measurements with further single and double polarization observables – as being planned and carried out at several laboratories – are urgently needed.**